3830 *Chem. Mater.* **2009,** *21,* 3830–3837
DOI:10.1021/cm9015063

CHEMISTRY OF MATERIALS
Article

Variable Lithium Coordination Modes in Two- and Three-Dimensional Lithium Boron Imidazolate Frameworks

Tao Wu,[†] Jian Zhang,[‡] Xianhui Bu,*[,‡] and Pingyun Feng*[,†]

[†]*Department of Chemistry, University of California, Riverside, California 92521, and* [‡]*Department of Chemistry and Biochemistry, California State University, 1250 Bellflower Boulevard, Long Beach, California 90840*

Received June 2, 2009. Revised Manuscript Received July 19, 2009

Despite years of efforts, known metal−organic frameworks rely predominantly on the use of group 12, d- and f-block elements. Recently, there has been a surge of interest in the use of s- and p-block elements (e.g., Mg and Al) as framework polyhedral nodes. Still, there are much fewer framework materials constructed from lightweight second-row elements (e.g., Li and B). Here we report three framework structures constructed by using lithium and boron as 3- or 4-connected nodes. It is shown that structural features of the poly(azolyl)borate anion can be used to induce 3-connected lithium sites, as compared to much more common 4-connected lithium sites. The creation of 3-connected lithium is of significance because it may offer open metal sites for enhanced guest binding. **BIF-10** is a 3-connected three-dimensional lithium boron imidazolate built from the tripodal $[BH(mim)_3]^-$ anion (mim = 2-methylimidazolyl). One unique feature of **BIF-10** is that lithium sites in two interpenetrating sublattices have different coordination numbers (tetrahedral with a terminating DMF molecule or trigonal planar). **BIF-11** built from the tetrahedral $[B(2,4\text{-dmim})_4]^-$ anion (2,4-dmim = 2,4-dimethylimidazolyl) possesses the sodalite-type framework and represents an ideal example that demonstrates the competitive structure-directing effect of two methyl substituents. **BIF-12** built from tetrahedral $[B(bim)_4]^-$ anion (bim = benzimidazolyl) has a 3-connected layer structure with a dangling bim group, revealing another way in which the structure of poly(azolyl)borate anions can induce the 3-connected lithium site.

Introduction

There is currently a strong interest in the synthesis of crystalline porous materials because of their potential applications in areas such as gas storage,[1−4] separation,[5−7] and catalysis.[8,9] Among these materials, metal−organic frameworks (MOFs) represent the latest addition. A survey of literature shows that the vast majority of reported porous MOFs are based on elements such as 3d metal cations[10−12] or

*To whom correspondence should be addressed. E-mail: pingyun.feng@ucr.edu (P.F.); xbu@csulb.edu (X.B.).

(1) (a) Murray, L. J.; Dincă, M.; Long, J. R. *Chem. Soc. Rev.* **2009**, *38*, 1294–1314. (b) Dinc, M.; Long, J. R. *Angew. Chem., Int. Ed.* **2008**, *47*, 6766. (c) Dinca, M.; Yu, A. F.; Long, J. R. *J. Am. Chem. Soc.* **2006**, *128*, 17153.
(2) (a) Rosi, N. L.; Eckert, J.; Eddaoudi, M.; Vodak, D. T.; Kim, J.; O'Keeffe, M.; Yaghi, O. M. *Science* **2003**, *300*, 1127. (b) Rowsell, J. L. C.; Millward, A. R.; Park, K. S.; Yaghi, O. M. *J. Am. Chem. Soc.* **2004**, *126*, 5666. (c) Millward, A. R.; Yaghi, O. M. *J. Am. Chem. Soc.* **2005**, *127*, 17998. (d) Han, S. S.; Furukawa, H.; Yaghi, O. M.; Goddard, W. A. *J. Am. Chem. Soc.* **2008**, *130*, 11580.
(3) (a) Zhao, D.; Yuan, D.; Zhou, H.-C. *Energy EnViron. Sci.* **2008**, *1*, 222–235. (b) Sun, D.; Ma, S.; Ke, Y.; Collins, D. J.; Zhou, H.-C. *J. Am. Chem. Soc.* **2006**, *128*, 3896–3897. (c) Wang, X.-S.; Ma, S.; Sun, D.; Parkin, S.; Zhou, H.-C. *J. Am. Chem. Soc.* **2006**, *128*, 16474–16475. (d) Ma, S.; Sun, D.; Simmons, J. M.; Collier, C. D.; Yuan, D.; Zhou, H.-C. *J. Am. Chem. Soc.* **2008**, *130*, 1012–1016.
(4) Pan, L.; Parker, B.; Huang, X. Y.; Olson, D. H.; Lee, J.; Li, J. *J. Am. Chem. Soc.* **2006**, *128*, 4180.
(5) (a) Li, J. R.; Kuppler, R. J.; Zhou, H.-C. *Chem. Soc. Rev.* **2009**, *38*, 1477–1504. (b) Ma, S.; Sun, D.; Wang, X.; Zhou, H.-C. *Angew. Chem., Int. Ed.* **2007**, *46*, 2458–2462.
(6) (a) Wang, B.; Cote, A. P.; Furukawa, H.; O'Keeffe, M.; Yaghi, O. M. *Nature* **2008**, *453*, 207. (b) Britt, D.; Tranchemontagne, D.; Yaghi, O. M. *Proc. Natl. Acad. Sci. U.S.A.* **2008**, *105*, 11623–11627.
(7) Mueller, U.; Schubert, M.; Teich, F.; Puetter, H.; Schierle-Arndt, K.; Pastré, J. *J. Mater. Chem.* **2006**, *16*, 626–636.
(8) (a) Ma, L. Q.; Abney, C.; Lin, W. B. *Chem. Soc. Rev.* **2009**, *38*, 1248–1256. (b) Wu, C.; Hu, A.; Zhang, L.; Lin, W. *J. Am. Chem. Soc.* **2005**, *127*, 8940. (c) Wu, C.; Lin, W. *Angew. Chem., Int. Ed.* **2007**, *46*, 1075.
(9) (a) Seo, J. S.; Whang, D.; Lee, H.; Jun, S. I.; Oh, J.; Jeon, Y. J.; Kim, K. *Nature* **2000**, *404*, 982. (b) Dybtsev, D. N.; Nuzhdin, A. L.; Chun, H.; Bryliakov, K. P.; Talsi, E. P.; Fedin, V. P.; Kim, K. *Angew. Chem., Int. Ed.* **2006**, *45*, 916. (c) Cho, S. H.; Ma, B. Q.; Nguyen, S. T.; Hupp, J. T.; Albrecht-Schmitt, T. E. *Chem. Commun.* **2006**, 2563. (d) Tanaka, K.; Oda, S.; Shiro, M. *Chem. Commun.* **2008**, 820.
(10) (a) Ma, L. Q.; Mihalcik, D. J.; Lin, W. B. *J. Am. Chem. Soc.* **2009**, *131*, 4610–4612. (b) Wu, S. T.; Ma, L. Q.; Long, L. S.; Zheng, L. S.; Lin, W. B. *Inorg. Chem.* **2009**, *48*, 2436–2442. (c) Wu, C. D.; Ma, L. Q.; Lin, W. B. *Inorg. Chem.* **2008**, *47*, 11446–11448. (d) Taylor, K. M. L.; Rieter, W. J.; Lin, W. B. *J. Am. Chem. Soc.* **2008**, *130*, 14358–14359. (e) Ma, L. Q.; Lin, W. B. *J. Am. Chem. Soc.* **2008**, *130*, 13834–13835.
(11) (a) Férey, G.; Mellot-Draznieks, C.; Serre, C.; Millange, F.; Dutour, J.; Surblé, S.; Margiolaki, I. *Science* **2005**, *309*, 2040–2042. (b) Férey, G.; Millange, F.; Morcrette, M.; Serre, C.; Doublet, M. L; Grenèche, J. M.; Tarascon, J. M. *Angew. Chem., Int. Ed.* **2007**, *46*, 3259–3263. (c) Hwang, Y. K.; Hong, D. Y.; Chang, J. S.; Jhung, S. H.; Seo, Y. K.; Kim, J. H.; Vimont, A.; Daturi, M.; Serre, C.; Férey, G. *Angew. Chem., Int. Ed.* **2008**, *47*, 4144–4148.
(12) (a) Rosi, N. L.; Kim, J.; Eddaoudi, M.; Chen, B. L.; O'Keeffe, M.; Yaghi, O. M. *J. Am. Chem. Soc.* **2005**, *127*, 1504. (b) Zhang, M. B.; Chen, Y. M.; Zheng, S. T.; Yang, G. Y. *Eur. J. Inorg. Chem.* **2006**, 1423. (c) Ma, C. B.; Chen, C. N.; Liu, Q. T.; Liao, D. Z.; Li, L. C.; Sun, L. C. *New J. Chem.* **2003**, *27*, 890. (d) Zhao, B.; Cheng, P.; Chen, X. Y.; Cheng, C.; Shi, W.; Liao, D. Z.; Yan, S. P.; Jiang, Z. H. *J. Am. Chem. Soc.* **2004**, *126*, 3012.
(13) (a) Taylor, K. M. L.; Jin, A.; Lin, W. B. *Angew. Chem., Int. Ed.* **2008**, *47*, 7722–7725. (b) Rieter, W. J.; Taylor, K. M. L.; An, H. Y.; Lin, W. L.; Lin, W. B. *J. Am. Chem. Soc.* **2006**, *128*, 9024–9025.

Published on Web 08/03/2009

4f elements[13−15] that are beyond the third period of the periodic table. Recently, there has been a surge of interest in using s- and p-block elements such as Mg, Al, and In as framework polyhedral nodes.[16−19] In particular, lightweight elements such as Mg and Al are considered highly desirable for constructing low-density MOFs with potential applications as on-board hydrogen storage materials.[16,17] In another effort toward low-density porous materials, a family of covalent organic frameworks (COFs with B, C, N, O) have also been reported.[20,21]

Being the lightest element capable of serving as polyhedral nodes, lithium is of outstanding interest for developing lightweight MOFs.[22] Furthermore, its high polarization ability may enhance the binding affinity for gas molecules. On the other hand, the high solvation energy of the lithium ion makes the crystallization of Li-MOFs highly challenging. Very recently, a new progress has been made in designing lithium-containing zeolite-type frameworks, resulting in four lithium boron imidazolates (i.e., **BIF-1**, **-2**, **-3**, and **-9** with topologies of *zni*, diamond, sodalite, and *RHO*, respectively). In all these compounds, lithium sites, as well as boron sites, exhibit the 4-connected tetrahedral coordination pattern, as is typical in zeolite-type structures.[23]

Metal sites that are coordinatively unsaturated are of particular interest because unused metal coordination sites may enhance the binding affinity between the host framework and guest molecules. Since the most common geometry for lithium is tetrahedral, the 3-coordinate lithium sites would be unsaturated and thus highly interesting. The 3-coordinate lithium sites can also be generated if the fourth coordination site is occupied by a removable solvent molecule.

Different from our earlier work on tetrahedral Li−B imidazolates, the work reported here probes two new aspects of the lithium boron imidazolate system. One is about synthetic or structural factors capable of inducing lithium sites that are coordinatively unsaturated or contain easily removable solvent molecules. In this work, we have identified two factors that clearly contribute to the generation of 3-connected lithium sites. These two factors are associated with the structure of the presynthesized poly(azolyl)borate complexes, which can be chemically controlled prior to the solvothermal crystal growth.

Another aspect of this work relates to the structure-directing effect of substituents on the imidazolate ring. In the metal−imidazolate chemistry, the effect of substituents on the framework topology has been well recognized. However, when two or more substituents are present, an intriguing question arises. Do these multiple substituents exhibit a synergistic and cooperative effect in controlling the final framework topology, or does each individual substituent exhibit the structural directing effect on the basis of its own preference? In the latter case where each individual substituent strives to exert its own topological control and thereby competes against each other, which substituent determines the outcome of crystallization? In this work, the use of 2,4-dimethylimidazolate provides a unique opportunity to study such competitive structure-directing effects when more than one substituent is present.

In the following, we report the synthesis, structure, and select properties of three lithium boron imidazolate frameworks (**BIF-10**, **-11**, and **-12**) made by systematically exploring various synthetic parameters. In addition to the use of different types of poly(imidazolyl)borate anions (both tripodal and tetrahedral), lithium precursors containing various hard and soft anions have also been explored and are found to be critically important to the crystallization process. Furthermore, because of the anticipated crystallization difficulty due to the high solvation energy of lithium ions in polar solvents, we have employed different types of mixed solvents containing two solvents with varying degrees of polarity so that hydrophilicity−hydrophobicity characteristics of the mixed solvent (and therefore solvation behavior of lithium ions) can be tuned through the solvent ratio. New open-framework BIFs synthesized here provide new insights into the synthetic and structural chemistry of the lithium boron imidazolate system.

Experimental Section

Materials and Methods. All reagents and solvents employed were commercially available and used as supplied without further purification. TGA was carried out on a TA SDT Q600

(14) Zhang, J.; Wu, T.; Chen, S. M.; Feng, P.; Bu, X. *Angew. Chem., Int. Ed.* **2009**, *48*, 3486–3490.
(15) (a) Chen, B.; Wang, L. B.; Xiao, Y. Q.; Fronczek, F. R.; Xue, M.; Cui, Y. J.; Qian, G. D. *Angew. Chem. Int. Ed.* **2009**, *48*, 500–503. (b) Chen, B.; Wang, L. B.; Zapata, F.; Qian, G. D.; Lobkovsky, E. B. *J. Am. Chem. Soc.* **2008**, *130*, 6718–6719.
(16) (a) Zhang, J.; Chen, S. M.; Zingiryan, A.; Bu, X. *J. Am. Chem. Soc.* **2008**, *130*, 17246–17247. (b) Zhang, J.; Chen, S. M.; Valle, H.; Wong, M.; Austria, C.; Cruz, M.; Bu, X. *J. Am. Chem. Soc.* **2007**, *129*, 14168–14169.
(17) (a) Dincă, M.; Long, J. R. *J. Am. Chem. Soc.* **2005**, *127*, 9376. (b) Rood, J. A.; Noll, B. C.; Henderson, K. W. *Inorg. Chem.* **2006**, *45*, 5521. (c) Loiseau, T.; Lecroq, L.; Volkringer, C.; Marrot, J.; Férey, G.; Haouas, M.; Taulelle, F.; Bourrelly, S.; Llewellyn, P. L.; Latroche, M. *J. Am. Chem. Soc.* **2006**, *128*, 10223. (c) Abrahams, B. F.; Hawley, A.; Haywood, M. G.; Hudson, T. A.; Robson, R.; Slizys, D. A. *J. Am. Chem. Soc.* **2004**, *126*, 2894. (d) Rood, J. A.; Boggess, W. C.; Noll, B. C.; Henderson, K. W. *J. Am. Chem. Soc.* **2007**, *129*, 13675.
(18) (a) Zhang, J.; Chen, S. M.; Wu, T.; Feng, P.; Bu, X. *J. Am. Chem. Soc.* **2008**, *130*, 12882–12883. (b) Zhang, J.; Chen, S. M.; Bu, X. *Angew. Chem., Int. Ed.* **2008**, *47*, 5434–5437.
(19) (a) Liu, Y. L; Kravtsov, V. Ch.; Beauchamp, D. A.; Eubank, J. F.; Eddaoudi, M. *J. Am. Chem. Soc.* **2005**, *127*, 7266. (b) Sun, J. Y.; Weng, L. H.; Zhou, Y. M.; Chen, J. X.; Chen, Z. X.; Liu, Z. C.; Zhao, D. Y. *Angew. Chem., Int. Ed.* **2002**, *41*, 4471. (c) Lin, Z. Z.; Jiang, F. L.; Yuan, D. Q.; Chen, L.; Zhou, Y. F.; Hong, M. C. *Eur. J. Inorg. Chem.* **2005**, 1927. (d) Lin, Z. Z.; Jiang, F. L.; Chen, L.; Yuan, D. Q.; Zhou, Y. F.; Hong, M. C. *Eur. J. Inorg. Chem.* **2005**, 77. (e) Gomez-Lor, B.; Gutierrez-Puebla, E.; Iglesias, M.; Monge, M. A.; Ruiz-Valero, C.; Snejko, N. *Chem. Mater.* **2005**, *17*, 2568.
(20) (a) Côté, A. P.; Benin, A. I.; Ockwig, N .W.; O'Keeffe, M.; Matzger, A. J.; Yaghi, O. M. *Science* **2005**, *310*, 1166–1170. (b) El-Kaderi, H. M.; Hunt, J. R.; Mendoza-Cortés, J. L.; Cté, A. P.; Taylor, R. E.; O'Keeffe, M.; Yaghi, O. M. *Science* **2007**, *16*, 268–272. (c) Cté, A. P.; El-Kaderi, H. M.; Furukawa, H.; Hunt, J. R.; Yaghi, O. M. *J. Am. Chem. Soc.* **2007**, *129*, 12914–12915.
(21) (a) Wan, S.; Guo, J.; Kim, J.; Ihee, H.; Jiang, D. *Angew. Chem., Int. Ed.* **2008**, *47*, 8826–8830. (b) Kuhn, P.; Antonietti, M.; Thomas, A. *Angew. Chem., Int. Ed.* **2008**, *47*, 3450–3453. (c) Tilford, R. W.; Mugavero, S. J.III; Pellechia, P. J.; Lavigne, J. *J. Adv. Mater.* **2008**, *20*, 2741–2746.
(22) (a) Banerjee, D.; Kim, S. J.; Parise, J. B. *Cryst. Growth Des.* **2009**, *9*, 2500–2503. (b) Knop, O.; Bakshi, P. K. *Can. J. Chem.* **1995**, *73*, 151.
(23) (a) Wu, T.; Zhang, J.; Zhou, C.; Wang, L.; Bu, X; Feng, P. *J. Am. Chem. Soc.* **2009**, *131*, 6111–6113. (b) Zhang, J.; Wu, T.; Zhou, C.; Chen, S.; Feng, P. *Angew. Chem., Int. Ed.* **2009**, *48*, 2542–2545.

Scheme 1. Reaction of 2-Methylimidazole with $NaBH_4$

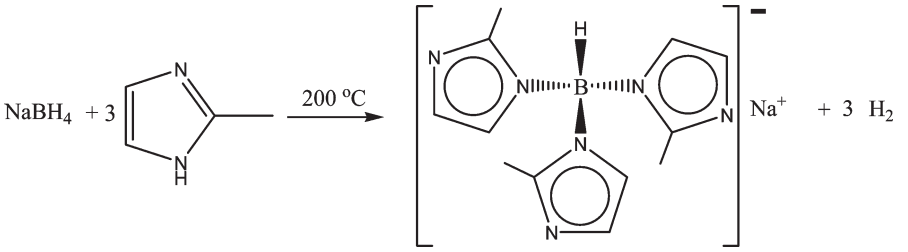

Scheme 2. Reaction of 2,4-Dimethylimidazole with $B(NMe_2)_3$

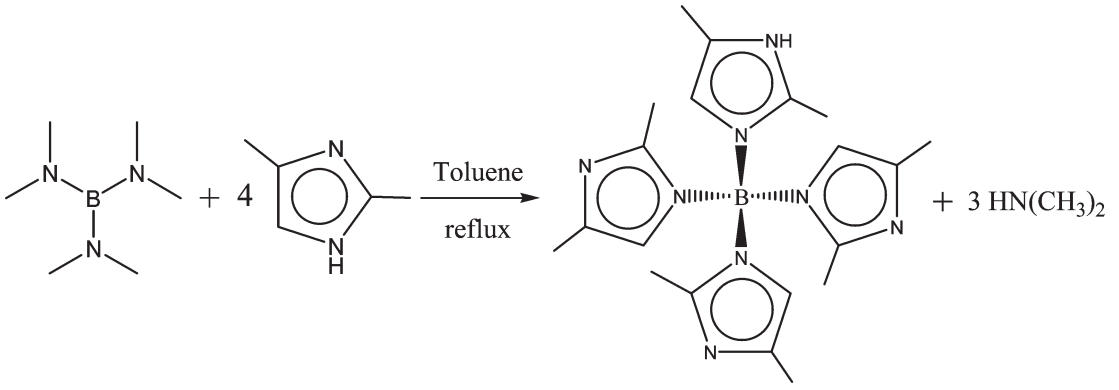

thermal analysis system with the heating rate of 10 °C/min from 30 to 1000 °C. Powder X-ray diffraction data were collected using a Bruker D8-Advance powder diffractometer operating at 40 kV, 40 mA for Cu Kα ($\lambda = 1.5406$ Å) radiation (2θ range, 5−40°; step size, 0.03°; scan speed, 60 s/step). Gas sorption experiments were carried out on a Micromeritics ASAP 2010 surface area and pore size analyzer.

Synthesis of Na[BH(2-mim)$_3$] (2-mim = 2-methylimidazolyl). The synthesis of this material was similar to the literature procedure.[24] In a 300 mL nitrogen-flushed flask attached to an oil bubbler, 0.532 g (14.1 mmol) of sodium borohydride was mixed with 2-methylimidazole (3.481 g, 42.4 mol). The mixture was heated and stirred at 200 °C for 24 h and then cooled to room temperature. The resulting off-white solid was washed with dry acetone (3 × 20 mL) and dry toluene (3 × 20 mL), respectively, and dried under reduced pressure at room temperature. The crude products (2.946 g) were directly used for the following synthesis without further purification. The reaction equation is shown in Scheme 1.

Synthesis of HB(2,4-dmim)$_4$ (2,4-dmim = 2,4-dimethylimidazolyl). The synthesis was based on the procedure in the reported literature.[25] A total of 3.720 g (0.0260 mmol) of $B(NMe_2)_3$ was added to a solution of 2,4-dimethylimidazole (10.000 g, 0.1040 mol) in anhydrous toluene (50 mL), and the resulting mixture was heated to flux for 24 h. The solvent was then removed under vacuum, and the product was washed with dry hexane (4 × 20 mL) and dried under reduced pressure at room temperature to give the raw product (7.253 g, yield 68.71%). The raw sample was directly used for the following synthesis without further purification. The reaction equation is shown in Scheme 2.

Synthesis of HB(bim)$_4$ (bim = benzimidazolyl). The ligand was prepared according to the procedure in the reported literature.[25]

(24) Trofimenko, S. *J. Am. Chem. Soc.* **1967**, *89*, 3170–3177.
(25) Bailey, P. J.; Lorono-Gonzales, D.; McCormack, C.; Millican, F.; Parsons, S.; Pfeifer, R.; Pinho, P. P.; Rudolphi, F.; Perucha, A. S. *Chem.—Eur. J.* **2006**, *12*, 5293–5300.

Synthesis of Li$_2$[BH(2-mim)$_3$]$_2$[DMF] (BIF-10). Sodium hydrotris(2-methylimidazolyl)borate (0.208 g), Li_2S (0.068 g), *N*,*N*-dimethylformamide (DMF, 1.846 mL), and acetonitrile (1.177 g) were placed in a 20 mL vial and stirred for half an hour. The sample was sealed and heated at 85 °C for 7 days and then cooled to room-temperature. After washing by acetonitrile, the pale-yellow crystals were obtained in the yield of 0.131 g (29.3% based on sodium hydrotris(2-methylimidazolyl)borate).

Synthesis of Li[B(2,4-dmim)$_4$] (BIF-11). HB(2,4-dimethylimidazolyl)$_4$ (202.0 mg), Li_2S (74.2 mg), (±)-2-amino-1-butanol (1.315 g), benzene (8.358 g), and acetonitrile (2.199 g) are mixed in a 20 mL vial and stirred for half an hour. The vial was then sealed and heated at 85 °C for 2 days, followed by cooling to room temperature. A large amount of colorless crystals (122.1 mg, 60.91% based on HB(2,4-dimethylimidazolyl)$_4$) were obtained. The crystals were washed using acetonitrile five times and ethanol twice and dried at 85 °C in air for other measurements.

Synthesis of Li[B(bim)$_4$][(±)-2-AB] (BIF-12). HB(benzimidazolyl)$_4$ (198 mg), butyllithium solution (0.5 mL, 2.5 M in hexanes), (±)-2-amino-1-butanol (2.602 g), and benzene (1.590 g) are mixed in a Teflon-lined autoclave and stirred for 1 h. The autoclave was then sealed and heated at 120 °C for 5 days, followed by cooling to room temperature. A large amount of colorless rhombus crystals (145.3 mg, 61.3% based on HB(benzimidazolyl)$_4$) were obtained. The crystals were washed by using acetonitrile (2 × 5.0 mL) and dried at room temperature in air for other measurements.

BIF-10, **-11**, and **-12** are soluble in water and alcohol. However, they are not soluble in other organic solvents, such as acetonitrile, benzene, or chloroform. Note: Butyllithium solution is very reactive and sensitive to moisture. The great care should be exercised in handling it.

Single-Crystal X-ray Crystallography. Single-crystal X-ray analysis was performed on a Bruker Smart APEX II CCD area diffractometer with nitrogen-flow temperature controller using graphite-monochromated Mo Kα radiation (λ = 0.71073 Å), operating in the ω and φ scan mode. Raw data collection and

Table 1. Summary of Crystal Data and Structural Refinement Result of BIF-*n*

	BIF-10	BIF-11	BIF-12
formula[a]	$Li_2[BH(2\text{-mim})_3]_2\cdot[DMF]$	$Li[B(2,4\text{-dmim})_4]$	$Li[B(bim)_4]\cdot[(\pm)\text{-2-AB}]$
FW	597.21	398.25	575.41
crystal system	monoclinic	cubic	monoclinic
space group	*Cc*	*P*-3*n*	$P2_1/c$
a, Å	13.6623(5)	16.3139(1)	12.4369(3)
b, Å	13.9688(6)	16.3139(1)	13.4869(3)
c, Å	18.0454(9)	16.3139(1)	17.8943(3)
α, deg	90.00	90.00	90.00
β, deg	111.235(3)	90.00	90.709(1)
γ, deg	90.00	90.00	90.00
V, Å^3	3210.1(2)	4341.76(5)	3001.27(11)
Z	4	6	4
d_{calcd}, g cm^{-1}	1.236	0.914	1.273
R_1, wR_2[b]	0.0960, 0.2684	0.0691, 0.2121	0.0548, 0.1596
net, V.S.[c]	2-fold, *ths*, $10_2.10_4.10_4$	SOD, 4.4.6.6.6.6	*fes*, (4.8.8)

[a] 2-mim = 2-methylimidazolyl; 2,4-dmim = 2,4-dimethylimidazolyl; bim = benzimidazolyl; DMF = *N*,*N*-dimethylformamide; (±)-2-AB = (±)-2-amino-1-butanol. [b] $R_1 = \sum||F_o|-|F_c||/\sum|F_o|$ and $wR_2 = \{\sum w(F_o^2-F_c^2)^2/\sum w(F_o^2)^2\}^{1/2}$. [c] For definitions of three-letter abbreviations and vertex symbol (V.S.), see Reticular Chemistry Structure Resource (http://rcsr.anu.edu.au/).

refinement were done using SMART. Data reduction was performed using SAINT$^+$ and corrected for Lorentz and polarization effects.[26] The SADABS program was used for absorption correction. The structure was solved by direct methods, and the structure refinements were based on $|F^2|$ with anisotropic displacement using SHELX-97.[27] All non-hydrogen atoms were refined with anisotropic displacement parameters. All hydrogen atoms were placed in calculated positions. All crystallographic calculations were conducted with the SHELXTL software suites. The crystallographic data and the structural refinement parameters were summarized in Table 1. CCDC-734220−734222 contain the supplementary crystallographic data, which can be obtained free of charge at www.ccdc.cam.ac.uk/conts/retrieving.html (or from the Cambridge Crystallographic Data Center, 12, Union Road, Cambridge CB21EZ, U.K.; fax (+44) 1223-336-033; or deposit@ccdc.cam.ac.uk).

Results and Discussion

Two-Step Synthesis Strategy and Importance of Lithium Precursors. To create new open-framework imidazolates, one effective method is to use poly(imidazolyl)borate anions with different substituents on the imidazolate ring. It has been demonstrated earlier that in the zinc imidazolate system, the type, number, and position of substituents on the imidazolate ring can alter framework topologies through the ligand−ligand steric interactions. However, unlike the zinc−imidazolate system in which zinc−imidazolate bonds are formed in situ from a zinc salt (e.g., zinc nitrate) and a neutral imidazole base during solvothermal synthesis, poly(imidazolyl)borate anions have not been found to form in situ in the solvothermal synthesis and therefore need to be prepared by chemical synthesis prior to solvothermal crystal growth. As illustrated in Schemes 1 and 2, two different methods were employed to synthesize poly(imidazolyl)borate anions. Both tripodal and tetrahedral forms ($Na[BH(2\text{-mim})_3]$, $HB(2,4\text{-dmim})_4$, $HB(bim)_4$) have been made in this work. These three different poly(imidazolyl)borate anions were subsequently used to prepare **BIF-*n*** ($n = 10-12$) through solvothermal reactions with a lithium salt.

The most unusual aspect of the solvothermal synthesis and crystallization is the critical effect of lithium precursors, or more specifically, the nature of counteranions in the lithium salt. A number of common lithium salts, such as $LiNO_3$, LiCl, LiOH, and $LiPF_6$, have been studied as lithium sources without any success. The use of these lithium salts usually gives rise to a clear solution or transparent gel after several days of solvothermal reactions. On the other hand, lithium salts that contain soft Lewis bases such as S^{2-} or R^- (alkyl groups such butyl) help to promote the crystallization of Li−B imidazolate frameworks. One possible reason is that S^{2-} or R^- is less likely to form ion pairs (or aggregates) with Li^+ in the reaction system, thereby making it more energetically favorable for Li^+ to bond with boron imidazolate anions. It is worth noting that the importance of sulfides or organometallic precursors in the synthesis of metal−organic framework materials has been very little appreciated until this work on Li−B imidazolates. It is conceivable that the use of such uncommon salts in other compositions may allow us to access new metal−organic framework materials.

Induction of 3-Connected Lithium Sites Using Tripodal Borate Anions in BIF-10. With our two-step synthetic strategy, the connectivity of poly(imidazolyl)borate anions can be controlled through the first-step chemical synthesis. As a result, both 3-connected tripodal anions (i.e., $[BH(2\text{-mim})_3]^-$) and tetrahedral anions (i.e., $[B(2,4\text{-dmim})_4]^-$, $[B(bim)_4]^-$) can be synthesized prior to the solvothermal assembly. In comparison, the coordination geometry of lithium ions in the final extended frameworks will need to be decided during the solvothermal reaction. On the basis of this study, it is clear that it is possible to use the specific types of poly(imidazolyl)borate anions to induce the coordination modes of lithium ions.

The first strategy to induce 3-connected lithium sites is through the use of the tripodal borate anion. During the solvothermal assembly of lithium ions with poly(imidazolyl)-borate anions, various topologies can be produced, including

(26) *SAINT*$^+$, version 6.22; Bruker Analytical X-Ray Systems, Inc.: Madison, WI, 2001.
(27) Sheldrick, G. M. *SHELX-97*; Bruker Analytical X-Ray Systems, Inc.: Madison, WI, 1997.

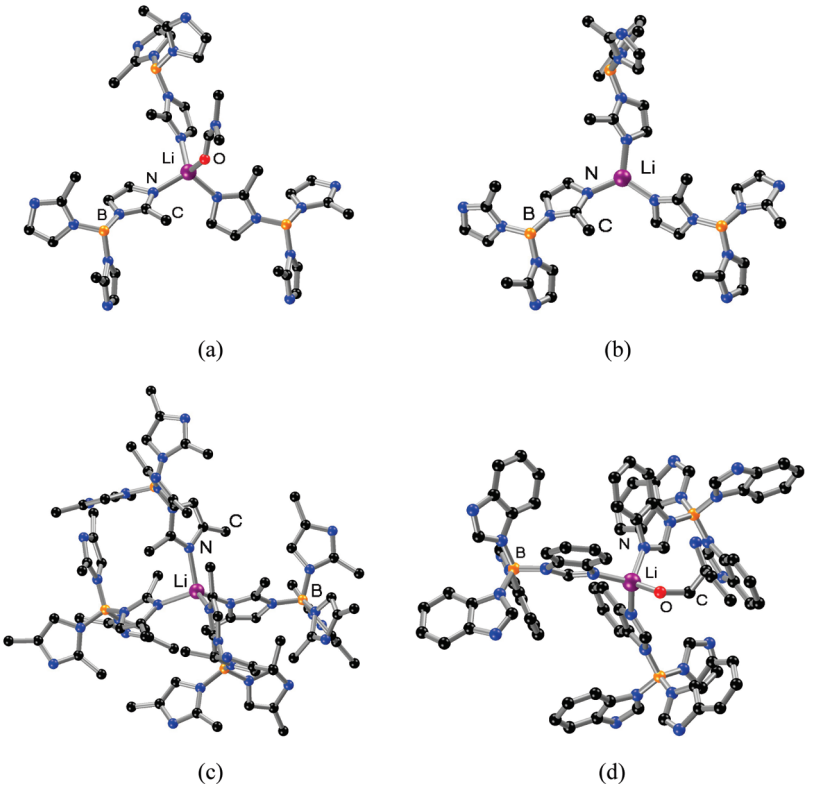

Figure 1. Coordination environment of Li^{I}. (a) Tetrahedral LiN_3O in **BIF-10** (b); trigonal planar LiN_3 in **BIF-10**; (c) tetrahedral LiN_4 in **BIF-11**; and (d) tetrahedral LiN_3O in **BIF-12**.

4-connected, mixed (3, 4)-connected, and 3-connected topologies. However, default topologies based on the mixed (3, 4)-connected or 3-connected nets are relatively few compared to 4-connected tetrahedral topologies. Therefore, if the connectivity of poly(imidazolyl)borate anions is 3-connected tripodal form so that 4-connected framework topologies are excluded, it should be possible to induce trigonal coordination in lithium ions (or tetrahedral coordination with a terminating solvent molecule). The 3-connected boron imidazolate anions are also likely to induce 3-connected lithium sites because a neutral framework would result.

X-ray single-crystal structure analysis shows that **BIF-10** crystallizes in noncentrosymmetric monoclinic space group *Cc*. The asymmetric unit includes two lithium ions, two hydrotris(2-methylimidazolyl)borate ligands, and one DMF molecule. Each boron atom is covalently bonded to three nitrogen atoms from 2-mim (B−N bond length 1.529−1.590 Å) and one hydride ion. Li1 adopts planar trigonal geometry to coordinate to three 2-mim ligands (Li−N bond length 1.943−2.046 Å). In contrast, Li2 is tetrahedrally linked to three 2-mim ligands (Li−N bond length 2.033−2.071 Å) and one oxygen atom from DMF molecule (Li−O bond length 2.059 Å), as shown in Figure 1a,b. As a result, each Li^{I} center is bridged to three B^{III} centers by 2-mim linkers with the Li···B distance ranging from 5.593 to 5.749 Å. The ligand $[BH(2\text{-mim})_3]^-$ exists in both *S* and *R* configurations (Figure 2). The three tripodal ligands linked to the same lithium ion have either two *S* and one *R* configurations or two *R* and one *S* configurations.

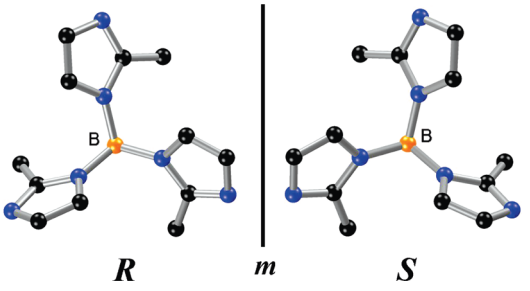

Figure 2. View of racemic tripodal $[BH(2\text{-mim})_3]^-$ ligands in **BIF-10**.

BIF-10 possesses 3-D 2-fold interpenetrating (10, 3)-*b* nets (also called the *ths* net) if both Li^{I} and B^{III} centers are regarded as 3-connected nodes. The most unusual feature in **BIF-10** is that one *ths* subnet (blue lines in Figure 3) contains only planar three-connected Li^{I} ions, while in the second *ths* net (green lines in Figure 3) all tetrahedrally coordinated Li^{I} ions are terminated by DMF molecules. Such structural features are in distinct contrast to a recently reported $Cu[BH(2\text{-mim})_3]$. This copper phase also exhibits 2-fold interpenetrating *ths* net;[23b] however, unlike **BIF-10**, two subnets in $Cu[BH(2\text{-mim})_3]$ possess exactly the same composition with identical coordination environment for the copper ion.

Competing Structure-Directing Effects of Two Methyl Groups in BIF-11. In contrast to trigonal-planar geometry for 50% lithium sites in **BIF-10** and tetrahedral coordination with one terminal solvent molecule for 50% lithium sites in **BIF-10** and 100% lithium site in **BIF-12**, lithium sites in **BIF-11** exhibit 4-connected tetrahedral geometry,

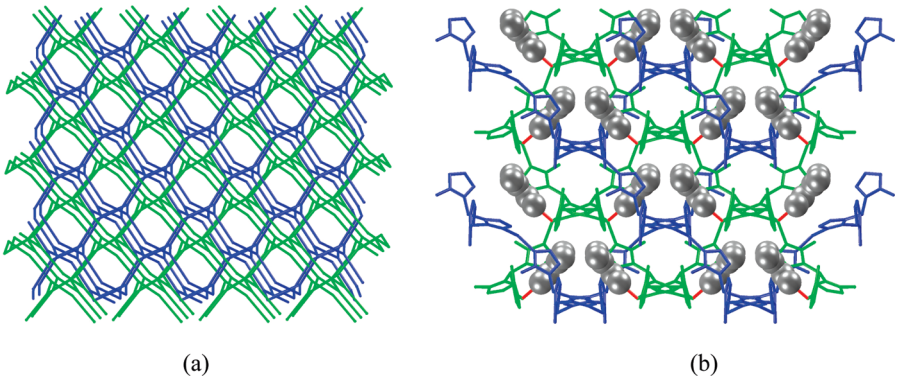

Figure 3. (a) 2-fold interpenetrating *ths* net in **BIF-10**; (b) only one subnet (green) containing DMF molecules (gray ball) is shown. The red bars represent O−Li bonds.

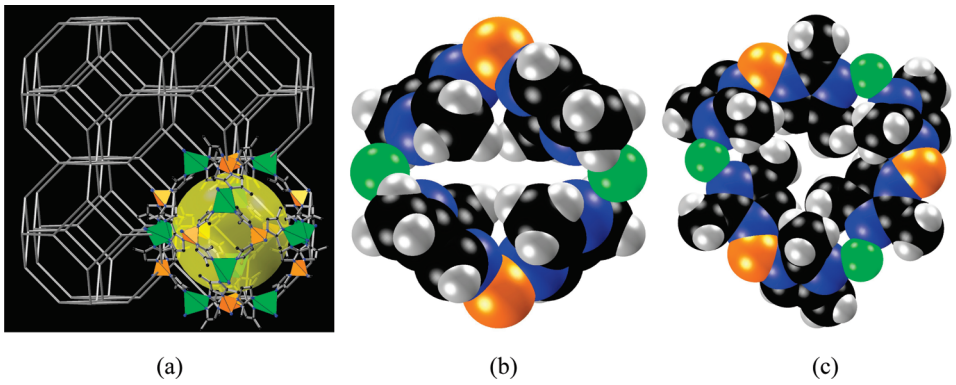

Figure 4. (Left) **SOD** topology of **BIF-11**; (middle) space-filling diagram of 4-ring $B_2Li_2(2,4\text{-dmim})_4$; (right) space-filling diagram 6-ring $B_3Li_3(2,4\text{-dmim})_6$. B in orange, N in blue, Li in green, C in black, and H in gray. The pore aperture sizes of 4-ring and 6-ring are too small to allow gas molecules to diffuse through.

leading to the zeolite-type sodalite topology. Of particular interest in **BIF-11** is the structure-directing effect of two competing methyl groups.

The unique insight that can be gained from **BIF-11** is that it suggests that each individual substituent can exhibit its own topological control during the solvothermal assembly. This can be seen by a comparison between **BIF-11** and two previously reported **BIFs**. It was reported earlier that monosubstitution by a methyl group at the 2-position leads to the formation of lithium boron imidazolate frameworks with the SOD topology while monosubstitution by a methyl group at the 4-position leads to the formation of lithium boron imidazolate frameworks with the RHO topology. Naturally, 2,4-dimethylimidazolate becomes especially interesting because it provides an opportunity for us to examine how these two methyl groups control the crystallization when they coexist in the same imidazolate. A large number of experiments have been performed using 2,4-dimethylimidazole under various reaction conditions, and **BIF-11** with the SOD topology is always obtained, suggesting that the methyl group at the 2-position dictates the crystallization process.

BIF-11 consists of one lithium ion and one-fourth of a tetrakis(2,4-dimethylimidazolyl)borate anion in the asymmetric unit of a highly symmetrical cubic space group *P*-3*n*. It exhibits a neutral 3-D tetrahedral framework in which each Li^I or B^{III} is tetrahedrally linked to four 2,4-dmim ligands (B−N bond length 1.551 Å; Li−N bond length 2.177 Å) and each 2,4-dmim linker bridges one Li^I and one B^{III} with the $Li^I\cdots B^{III}$ distance of 5.768 Å (Figure 1c). This 4-connected net with alternating Li and B tetrahedral nodes has an uninodal zeolite sodalite (SOD) topology (Figure 4a). Salient features of the SOD topology include β cages with 24 vertices and 4- and 6-ring (i.e., 4 or 6 tetrahedral sites) windows. Each β cage is connected to 14 other β cages by sharing 4-ring and 6-ring to form a 3-D framework (Figure S1, Supporting Information).

Three-Connected Lithium Sites Induced by Large Substituents in Tetrahedral Boron Imidazolate Anions in BIF-12. BIF-10 illustrates that 3-connected boron imidazolate anions (i.e., tripodal $[BH(im)_3]^-$) can induce 3-connected lithium sites. **BIF-12** shows that a large substituent in the tetrahedral $[B(bim)_4]^-$ anion can lead to 3-connected boron sites, which in turn induces the 3-connected lithium sites. This is primarily because of one unique aspect of the Li−B imidazolate system, which is the short B−N bond length (≈1.5 Å) between boron and the imidazolyl group (as compared to metal−ligand distances in other structures, usually 1.9 Å or larger).

In the previously reported Zn−imidazolate system, the imidazolate ligand−ligand interaction is known to play a key role in the resultant framework topology. The shorter B−N distance in the boron imidazolate system leads to a significantly closer distance between the adjacent ligand groups, which can further increase the steric repulsion

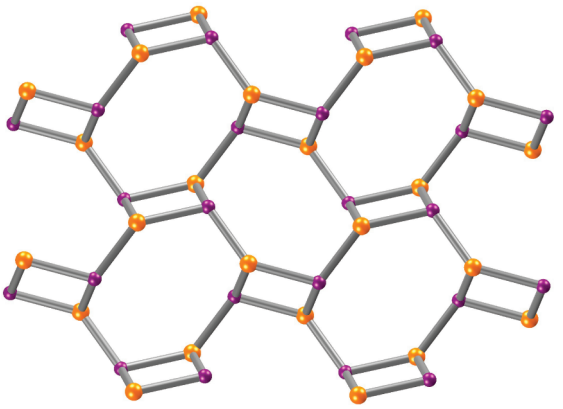

Figure 5. 2-D (4.8^2) *fes* topology in **BIF-12** (boron, orange; purple, lithium).

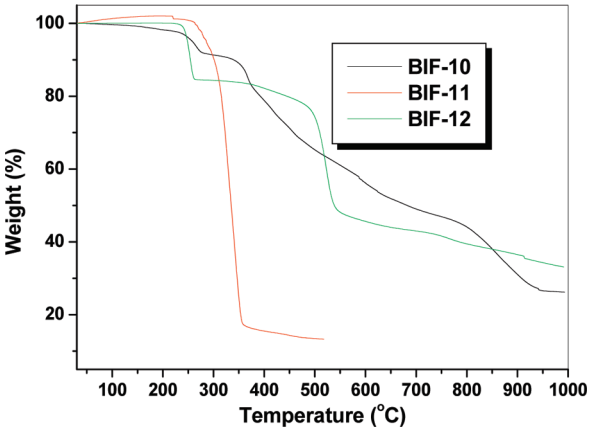

Figure 6. Thermogravimetric plots for **BIF-10**, **-11**, and **-12**.

between substituent groups on imidazolyl rings. Indeed, while benzimidazole is well-known to form the zeolite RHO type topology with zinc, the short B−N distance, coupled with the large benzo group, makes it sterically unlikely to form the RHO topology in the boron system when benzimidazole is used in the boron-centered anion. In **BIF-12**, the interligand steric repulsion contributes to the formation of a layer structure with 3-connected boron and lithium sites.

BIF-12 consists of one lithium ion, one tetrakis(benzimidazolyl)borate anion, and one (±)-2-amino-1-butanol solvent molecule in its asymmetric unit. Unlike tetrahedral $[B(2,4\text{-dmim})_4]^-$ anion in **BIF-11**, each tetrahedral $[B(bim)_4^-]$ anion only bonds to three Li^I sites through the nitrogen donor of three benzimidazolyl groups, and the fourth benzimidazolyl is a terminating ligand. Similar to the Li-DMF coordination in **BIF-10**, Li^I adopts LiN_3O tetrahedral coordination geometry with a terminal solvent molecule (±)-2-AB (Figure 1d). **BIF-12** possesses a 2-D wavy (4.8.8) layer (also called *fes* net) (Figure 5), in which the racemic solvent molecules (±)-2-AB are spontaneously separated onto adjacent lithium sites (Figure S2, Supporting Information). A recently reported Cu[BH(im)$_3$] (im = imidazolyl) complex also exhibits *fes* net;[23b] however, unlike **BIF-12**, this copper compound does not contain terminal solvent molecules, highlighting some difference in the chemistry of lithium and copper ions.

Variable Lithium Coordination Modes from BIF-10 to BIF-12. It is of interest to note that the coordination modes in **BIF-10**, **-11**, and **-12** are all different. Three different modes can be identified: (1) tetrahedral 4-connected mode in **BIF-11**, (2) tetrahedral 3-connected mode for 50% lithium sites in **BIF-10** and 100% lithium sites in **BIF-12**, and (3) trigonal-planar mode for 50% lithium sites in **BIF-10**. Furthermore, it is possible to correlate such variable lithium coordination modes with other parameters. One of the most important factors in determining the coordination mode of lithium sites is the structure of boron imidazolate anions, as discussed above. However, the solvent property and lithium precursors also play essential roles in the crystallization process. The hard Lewis acid character and large solvation energy of the lithium ion create unique challenges as well as opportunities in the preparation of lithium open-framework materials, as illustrated by the success in the synthesis of three lithium boron imidazolate structures reported here.

Thermal Properties and Gas Adsorption Characteristics. To verify whether the frameworks of **BIF-*n*** are maintained after the removal of dangling solvent molecules, TGA and X-ray powder diffraction (XRPD) were used to investigate the framework stability. The TGA result of **BLF-10** carried out under N_2 (Figure 6) reveals that there is a weight loss of nearly 10.10% from room temperature to 280 °C, followed by a short plateau. The observed weight loss is attributed to the loss of most solvent DMF molecules (12.24%, calcd). The XRPD pattern of the desolvated solid prepared by heating at 280 °C under vacuum for 40 h is nearly identical to the simulated pattern and the pattern of the as-synthesized sample (Figure S3, Supporting Information), suggesting the stability of **BIF-10** toward partial solvent loss. However, gas uptakes of N_2, H_2, or CO_2 indicate the desolvated sample of **BIF-10** is nonporous, which might be due to the small aperture size (Figure S4, Supporting Information).

TGA and the XRPD pattern (Figure S5, Supporting Information) show that the **BIF-11** with the SOD structure is stable up to approximately 200 °C. However, gas sorption measurements on N_2, H_2, and CO_2 show that **BIF-11** is nonporous despite the large internal pore space within the sodalite cage (Figure S6, Supporting Information). This is likely because the apertures of 6-ring and 4-ring windows are blocked by methyl groups at the 4-position, resulting in an aperture size smaller than the kinetic diameter of gas molecules (2.89 Å) (Figure 4b,c). Note that as demonstrated by **BIF-3** with the sodalite structure, the lack of porosity in **BIF-11** is unlikely due to the methyl group at the 2-position. Thus, while the methyl group at the 4-position exhibits no structure-directing effect on the framework topology, it does affect the porosity of the resulting material.

The thermogravimetric analysis on **BIF-12** shows a weight loss of 15.48%, which is in good agreement with calculated value (15.49%) for the loss of solvent molecules (Figure S7, Supporting Information). Interestingly, the XRPD pattern of the desolvated **BIF-12** treated at 270 °C

under reduced pressure indicates a new highly crystalline phase. This suggests that a solid−solid phase transformation has occurred. It is suggested that upon the loss of solvent molecules, there is a further cross-linking between open lithium sites and dangling benzimidazolate ligands on the boron site. The cross-linking could occur within the layer, which would result in the formation of a 4-connected square-grid-like layer structure ($Li[B(bim)_4]$, denoted as **BIF-13** here) reported earlier.[23a] However, The XRD pattern of thermally treated **BIF-12** is not exactly the same as that of **BIF-13**, which was solvothermally prepared at a higher temperature (150 °C, as compared to 120 °C for **BIF-12**).[23a] Alternatively, it is also possible that the adjacent layers could be cross-linked following the solvent loss, leading to a three-dimensional topology. Unfortunately, the product from the thermal transformation of **BIF-12** could not be established by single-crystal X-ray diffraction due to the small crystal size.

Conclusion

Reported here are three imidazolate framework structures constructed by using lightweight lithium and boron as 3- and 4-connected nodes. In addition to demonstrating a competitive structure-directing effect by substituents on imidazolate rings, we highlight two different structural features of boron imidazolate anions that serve to induce 3-connected lithium sites, as compared to more common 4-connected lithium sites. The creation of 3-connected lithium sites is of significance because of its potential to serve as open metal sites for enhanced binding to gas molecules. The results from this work should be useful in the further development of lithium-based open-framework materials with variable coordination modes and useful gas sorption properties.

Acknowledgment. We thank the support of this work by the NSF (P.F., CHEM-0809335, X.B., DMR-0846958). P.Y. is a Camille Dreyfus Teacher Scholar and X.B, is a Henry Dreyfus Teacher Scholar.

Supporting Information Available: Additional structural figures, XRPD patterns, sorption isotherms, and optical image of BIF-11 crystals (PDF); crystallographic data including positional parameters, thermal parameters, and bond distances and angles (CIF). This material is available free of charge via the Internet at http://pubs.acs.org.